110–120 *Nucleic Acids Research, 2008, Vol. 36, No. 1* *Published online 13 November 2007*
doi:10.1093/nar/gkm759

Dynamic structures of *Bacillus subtilis* RecN–DNA complexes

Humberto Sanchez[1,2], Paula P. Cardenas[1], Shige H. Yoshimura[2], Kunio Takeyasu[2] and Juan C. Alonso[1,*]

[1]Departamento de Biotecnología Microbiana, Centro Nacional de Biotecnología, CSIC, Campus Universidad Autónoma de Madrid, Darwin 3, Cantoblanco, 28049 Madrid, Spain and [2]Laboratory of Plasma Membrane and Nuclear Signalling, Graduate School of Biostudies, Kyoto University, Sakyo-ku, Kitashirakawa-Oiwake-cho, Kyoto 606-8502, Japan

Received July 20, 2007; Revised September 10, 2007; Accepted September 11, 2007

ABSTRACT

Genetic and cytological evidences suggest that *Bacillus subtilis* RecN acts prior to and after end-processing of DNA double-strand ends via homologous recombination, appears to participate in the assembly of a DNA repair centre and interacts with incoming single-stranded (ss) DNA during natural transformation. We have determined the architecture of RecN–ssDNA complexes by atomic force microscopy (AFM). ATP induces changes in the architecture of the RecN–ssDNA complexes and stimulates inter-complex assembly, thereby increasing the local concentration of DNA ends. The large CII and CIII complexes formed are insensitive to SsbA (counterpart of *Escherichia coli* SSB or eukaryotic RPA protein) addition, but RecA induces dislodging of RecN from the overhangs of duplex DNA molecules. Reciprocally, in the presence of RecN, RecA does not form large RecA–DNA networks. Based on these results, we hypothesize that in the presence of ATP, RecN tethers the 3′-ssDNA ends, and facilitates the access of RecA to the high local concentration of DNA ends. Then, the resulting RecA nucleoprotein filaments, on different ssDNA segments, might promote the simultaneous genome-wide homology search.

INTRODUCTION

All cells have systems dedicated to correct DNA damage, although if lesions are left unrepaired removal of single-strand (ss) DNA gaps by homologous recombination (HR) or removal of double-strand breaks (DSBs) via HR or non-homologous end joining (NHEJ) are the ultimate resource for the re-establishment of the replication fork (1–7).

Cytological experiments have documented the assembly of large nucleoprotein complexes that contain DNA-repair proteins in response to DNA damage (8–10). The mammalian Mre11–Rad50–Nbs1 (MRN) and budding yeast Mre11–Rad50–Xrs2 (MRX) complex [simplified as MRN(X) complex] are the early DSB sensors during mitotic recombination (5,8,10). It has been proposed that MRN(X) complexes act at the branching point upstream of both HR and NHEJ (11,12). The DNA ends are transiently stabilized, and there is a window of opportunity for NHEJ to occur. However, once the DNA ends are resected, the cell is committed to HR and NHEJ is no longer an option (6,7,11,12).

The overall structure of the structural maintenance chromosome (SMC) protein Rad50 is evolutionary conserved from bacteria to humans. Bioinformatic studies suggest that bacterial SbcCs, SMC and RecN proteins share a similar modular organization with eukaryotic Rad50, a bipartite globular ATPase domain made up from the N- and C-termini of the protein separated by an extensive central region predicted to form a coiled-coil (13,14; Figure 1). Furthermore, the structural conservation of RecF and Rad50 suggests a conserved mechanism of action (15). However, a clear spatial and temporal distinction between the localization of RecN, RecF, SMC and SbcC proteins was reported (16–18).

In *Bacillus subtilis* two-ended DSBs are mainly repaired via HR, but with very low efficiency also by NHEJ (4,18). Genetic studies revealed that SbcC is epistatic with Ku (a key component of NHEJ) (19), but they are non-epistatic with RecN, suggesting that RecN and Ku/SbcC define different avenues for DSB repair (18). RecN promotes the assembly of large nucleoprotein complexes that contain recombination proteins in response to DNA damages. In *B. subtilis* cells, 15 min after induction of a site-specific DSB or randomly introduced DSBs a massive reorganization of the nucleoid takes place, and RecN

*To whom correspondence should be addressed. Tel: +34 91585 4546; Fax: +34 91585 4506; Email: jcalonso@cnb.uam.es

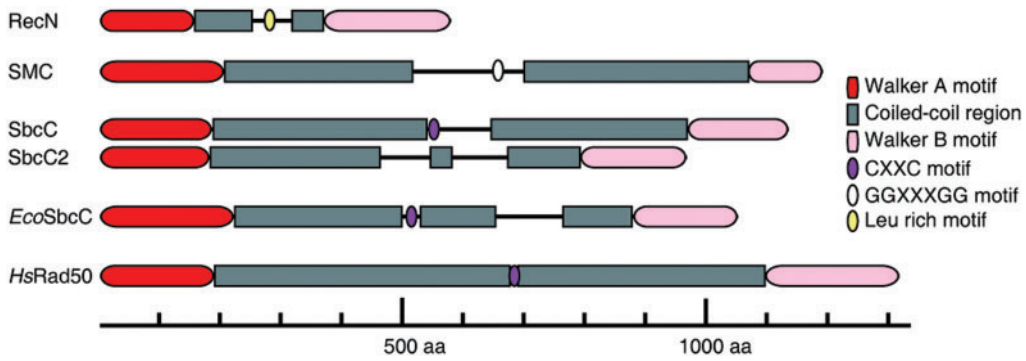

Figure 1. Secondary structure prediction and motifs of *B. subtilis* SMC-like proteins. The secondary structure *B. subtilis* SMC-like proteins [SMC, RecN, SbcC (also termed YirY) and SbcC2 (YhaN)] and its comparison with *E. coli* SbcC (*Eco*SbcC) and human Rad50 (*Hs*Rad50) were predicted using the COILS program (www.ch.embnet.org/software/COILS_form.html). The Walker A and B motifs and the CXXC and GGXXXGG motifs necessary for dimerization of Rad50, SbcC, *Eco*SbcC and SMC proteins, respectively, are indicated. The putative dimerization (Leu rich) motif of RecN is also indicated. Abbreviation: aa, aminoacids.

establishes a discrete DNA repair centre (RC) (17,20). Recombination proteins localize differentially to a RecN-induced RC: RecO, RecR and RecA are recruited 30–45 min after induction of DSBs, RecF (60 min) and RecU (120 min) are recruited at a RecN-directed RC at later stages, whereas others [e.g. AddAB (analogue of *Escherichia coli* RecBCD), RecG, RecS, DNA polymerase I] do not form discernible cytological foci (17,20,21). In the absence of end-processing functions (*addAB* Δ*recJ* strain) two to three (rather than one) RecN foci are formed, whereas RecA assembly at the RC is not observed (21). These observations suggest that RecN acts: (i) upstream of end-processing enzymes, perhaps as an early detector of DSBs, and (ii) after end-processing because the activity of the AddAB and/or RecJ exonucleases are required for the formation of one discrete RecN RC, and for RecA assembly at a RecN-directed RC (17,20,21). Furthermore, RecF failed to form foci in the absence of RecO, arguing that RecF, which shares structural conservation with the head domain of Rad50 (15), might work after RecA loading onto ssDNA.

During natural genetic recombination, the DNA uptake proteins localize to a cell pole (22), and RecN protein oscillates between the poles of competent *B. subtilis* cells (23). The internalized ssDNA stops the RecN oscillations, and then threads of RecA are seen to emanate from the pole (23). It is likely that RecN interacts *in vivo* with incoming ssDNA molecules and thereby is localized at the pole containing the natural competence machinery.

RecN also possesses biochemical activities associated with the eukaryotic MRN(X) complex (6,7,12,24). The globular N- and C-terminal regions of RecN should interact to form the active ATPase (25). *In vitro* RecN is a ssDNA-dependent ATPase and shows significant ATP-independent DNA binding. However, in the presence of a nucleotide cofactor (ATP or ADP), RecN binds specifically to 3′-OH termini forming large RecN–ssDNA networks that are not disrupted in the presence of an excess of ssDNA molecules (25).

Here, we report the visualization of dynamic complexes formed by RecN with ssDNA or duplex molecules containing internal ssDNA regions. Atomic force microscopy (AFM) has confirmed that RecN binds to ssDNA regions and, in the presence of ATP, the interactions between individual ssDNA–RecN complexes favour inter-complex association and result in large nucleoprotein complexes. The pre-formed ssDNA–RecN–ATP–Mg^{2+} aggregates are insensitive to the addition of SsbA (counterpart of *E. coli* SSB or eukaryotic RPA protein), arguing that RecN should bind ssDNA prior or concomitantly with SsbA. Independent of the order of addition, RecA promotes the disassembly of the pre-formed ssDNA–RecN–ATP–Mg^{2+} complexes and promotes DNA strand exchange without the formation of large RecA–DNA networks. We propose that RecN-promoted RCs facilitate RecA-promoted genome-wide homology search of the RecA pre-synaptic filaments.

MATERIALS AND METHODS

Enzymes reagents and protein purifications

RecN, RecA and SsbA proteins were purified as described (17,26, Carrasco *et al.*, unpublished data). The molar extinction coefficient for RecN, RecA and SsbA were calculated to be 30 600, 15 200, 11 400/M/cm at 280 nm as previously described (26). Protein concentrations were determined using the above molar extinction coefficients. RecN and RecA are expressed as moles of protein monomers and SsbA as tetramers.

Alkali lysis purified pBluescript DNA was linearized by EcoRI (NEB) digestion, and CsCl-purified pBluescript DNA was linearized by EcoRV (NEB) digestion. The 60-nt ssDNA molecule ($ssDNA_{60}$) used has been previously described (25). DNA concentrations were established using molar extinction coefficients using 8780 and 6500/M/cm at 260 nm for ssDNA and dsDNA, respectively. Unless otherwise stated, DNA concentrations are given as moles of nucleotides.

AFM Analysis

Aliquots of protein solutions, diluted in buffer A (10 mM HEPES, pH 7.5, 2 mM $MgCl_2$), were spotted onto a freshly cleaved mica substrate pre-treated with 10 mM

spermidine. After 2 min, at room temperature, the mica was washed several times with MilliQ water and dried under nitrogen. AFM observations were performed using a Nanoscope IIIa or IV microscope (Veeco) in air using Tapping Mode. The cantilever (OMCL-AC160TS-W2, Olympus) was 129 mm in length with a spring constant of 33–62 N/m. The scanning frequency was 2–3 Hz, and images were captured with the height mode in a 512×512 pixel format. The obtained images were plane-fitted and flattened by the computer program accompanying the imaging module.

We have assumed that the RecN-active ATPase has a globular domain. Based on the molecular mass of RecN (576 residues long, 64.4 kDa), we estimated the mass of the ATPase head domain of RecN monomers to be ~40 kDa taking into account the hydration component (see subsequently), and expected a volume of ~75 nm^3 when measuring by AFM. The interactions of the putative globular N- and C-terminal regions might extrude the intervening coiled-coil region as a tail (Figure 1). However, we did not observe such tails and the particle sizes were larger than expected for just the globular domains, suggesting that the central connecting region also contributed to the total particle volume (data not shown).

In the geometrical analyses of AFM images of DNA and protein, the 'tip effect' was removed by using the apparent size of DNA as a reference as described elsewhere (27,28). Briefly, the apparent dimensions of the molecules obtained by AFM are dependent upon the radius of the tip curvature and are apparently larger than the real dimensions. The relationship among the width of the globular molecule in the AFM image (W), the radius of the tip curvature (R_c) and the radius of the molecule (R_m) is given by $W = 4(R_c R_m)^{1/2}$. When two different molecules with R_{m1} and R_{m2} radii are imaged with the same tip, the relationship between the measured widths (W_1 and W_2) can be given by $W_1 = W_2(R_{m1}/R_{m2})^{1/2}$. Since the diameter of a dsDNA molecule is known (2 nm), we used the established parameter in our AFM image calculations as W_1. We could then calculate the radius of the particles (R_{m2}) from the apparent width of the DNA (W_2).

EMSA experiments

Reaction mixtures that contained [γ-^{32}P]-ssDNA$_{60}$ (60 nM in nt) and RecN (10 nM) were assembled in buffer B [50 mM Tris–HCl (pH 7.5), 50 mM NaCl, 2 mM $MgCl_2$, 1 mM DTT, 2% PEG-6000] for 10 min at 37°C, then the second protein [SsbA (100 nM), RecA (40 nM)] and 10 min later ADP or ATP (1 mM) was added and incubation continued for 10 min at 37°C. In some studies, SsbA or RecA was added to pre-formed ssDNA–RecN–ATP/ADP–Mg^{2+} complexes. The complexes formed were separated by polyacrylamide gel electrophoresis and visualized by phosphorimaging as previously described (25).

DNA substrates and binding reactions

EcoRI-cleaved pBluescript DNA (2986-bp) was partially digested with λ Exo (Invitrogen) to generate short 3′-ssDNA tails (linear duplex DNA with short ssDNA tails). EcoRV-cleaved pBluescript was exposed to Nt.AlwI endonuclease (NEB) to obtain blunt-ended DNA molecules with internal single-strand nicks. Protein–DNA complexes for AFM visualization were assembled as described for EMSA (25) and were deposited and imaged as described earlier.

Linear duplex DNA with short ssDNA tails (150 nM) and RecN (10 nM) were pre-incubated for 10 min at 37°C in buffer C [50 mM Tris–HCl (pH 7.5), 50 mM NaCl, 10 mM magnesium acetate, 50 μg/ml bovine serum albumin (BSA), 1 mM DTT], then ATP or ATPγS (1 mM) was added and incubation continued for 10 min at 37°C. To pre-formed ssDNA–RecN–ATP–Mg^{2+} or ssDNA–RecN–ATPγS–Mg^{2+} complexes, homologous circular plasmid DNA (150 nM) and RecA (40 nM) protein were added, and after incubation for 10 min at 37°C the complexes were spotted on freshly cut mica. Linear duplex DNA with short ssDNA tails (150 nM), RecA (40 nM) and 1 mM ATP were pre-incubated for 10 min at 37°C in buffer C and then homologous circular plasmid DNA (150 nM) was added, and after incubation for 10 min at 37°C the complexes were spotted on freshly cut mica.

RESULTS

AFM visualization and quantification of RecN binding to ssDNA

We were unable to detect formation of RecN–dsDNA complexes in EMSA using dsDNA segments up to 60-bp long (25). Alkali-lysed 2958 bp plasmid DNA was linearized with EcoRI to render molecules that were ~950 nm in length as determined by AFM (Figure 2A). RecN was occasionally seen bound at random sites along the duplex DNA molecules. The linearized DNA was subjected to limited λ exonuclease (λ Exo) digestion to obtain dsDNA molecules with 3′-ssDNA extensions of about 150–450 nt single-stranded regions at both termini (Figure 2B). RecN was able to bind these ssDNA extensions (Figure 2C, left panel). To gain information on the volume of RecN–DNA complexes, the diameter (d = width) of the RecN particles bound to the DNA were measured and plotted against the width of the DNA molecule to which they were bound. Linear regression adjustment of the data produced a line with an identical slope if dimeric species ($d = 5.7$ nm calculated diameter) were bound to the DNA ($d = 2$ nm)(27) (Figure 2C, right panel).

RecN molecules were also occasionally seen bound at random sites along the DNA molecules. It seemed possible that RecN, therefore, also binds, albeit with low efficiency to dsDNA or, more likely, the DNA molecules purified by the alkali-lyses method contained internal single-strand nicks that were enlarged by the λ Exo treatment. To address this, complexes formed with these DNA preparations and a genuine ssDNA-specific binding protein, SsbA, were also visualized by AFM. SsbA bound primarily to the λ Exo-generated 3′-ssDNA extensions but also infrequently to random sites along the linear

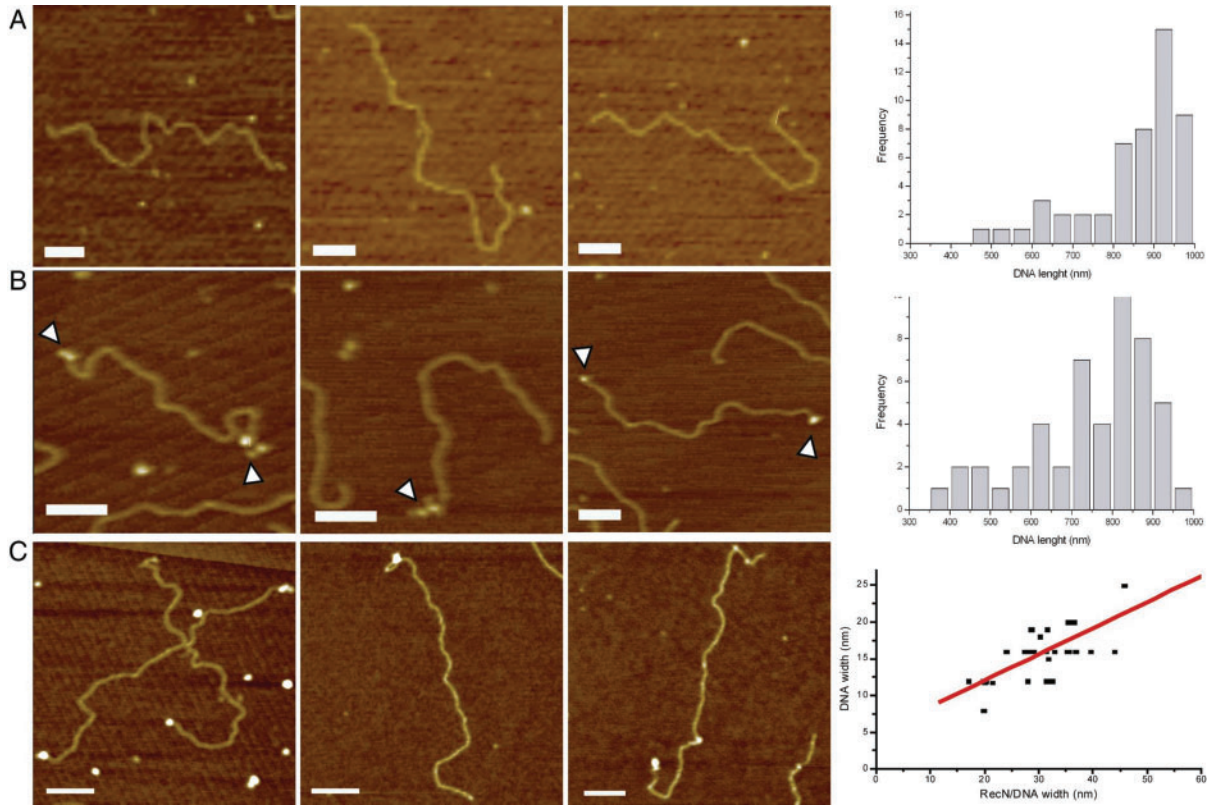

Figure 2. RecN binds short ssDNA tails in a duplex molecule. (**A**) Linear DNA (150 nM in nt) was incubated for 10 min at 37°C and deposited on freshly cut mica. (**B**) Linear DNA (150 nM) treated with λ Exo under limiting conditions and then incubated for 10 min at 37°C and deposited on freshly cut mica. White arrowheads highlight the presence of ssDNA tails in the linear plasmids. (**C**) Linear DNA (150 nM) with short ssDNA tails and RecN (10 nM) were incubated for 10 min at 37°C and deposited on freshly cut mica. Pictures show representative individual molecules. The graph shows the multimerization state of DNA-bound RecN complex. The sizes of the RecN complex bound to the ends of the DNA substrate were plotted against the width of bare DNA in the same image. The line shows the linear fitting of the data ($y = 4.97 + 0.35X$; $R = 0.82$). Scale bar = 100 nm.

DNA molecules (Supplementary Figure S1), arguing for the presence of internal ssDNA regions. Based on the sizes of the internal SsbA complexes, the regions of ssDNA are sufficient to accommodate a SsbA tetramer (29; Supplementary Figure S1).

Localization of RecN binding by endonuclease nicking of DNA

CsCl-purified plasmid DNA was linearized with EcoRV to obtain blunt-ended linear dsDNA molecules. DNA aliquots were exposed to Nt.AlwI, which introduced asymmetric site-specific nicks, and then RecN was added. AFM revealed RecN bound to <10% of control dsDNA molecules that had not been subjected to Nt.AlwI digestion, but to essentially all the Nt.AlwI digested DNA molecules. The asymmetry in the Nt.AlwI generated nicking sites, four on the plus strand and six on the minus strand (Figure 3B, top and bottom line, respectively), allowed us to landmark the relative position of the DNA ends. Measurements from the ends of the DNA molecules, confirmed that RecN molecules were positioned predominantly at the site where Nt.AlwI introduced ssDNA nicks (Figure 3A). RecN also bound to other sequences that have a propensity to form ssDNA bubbles (namely dA–dT rich regions associated with DNA unwinding elements linked to phage f1 and plasmid replication origins). Alternatively, RecN may also bind to dA–dT rich regions on dsDNA, although RecN did not seem to bind preferentially to the upstream dA–dT rich regions of the *lac* promoter (Figure 3B), suggesting that ssDNA rather than dA–dT rich region is the main target of RecN in the absence of ATP. This is consistent with the observations that RecN binds *in vivo* to take up ssDNA during natural transformation (see Introduction section), and RecN cannot bind duplex DNA lacking dA–dT rich pockets.

ATP-dependent aggregation of RecN–ssDNA complexes

It was shown in the previous section that in the absence of a nucleotide co-factor RecN has no strong preference for ssDNA ends over internal sites. Using EMSA, we found that in the presence of ATP, RecN assembles to form large networks with ssDNA molecule and requires 3′-OH at the ends of the ssDNA molecules (25). To investigate the interaction of RecN protein with 3′-ssDNA-tailed duplex DNA, 1 mM ATP was added to the pre-formed RecN–3′-ssDNA-tailed complex, the reaction was incubated for 20 min at 37°C, and observed by AFM. Figure 4 shows different scenarios with different

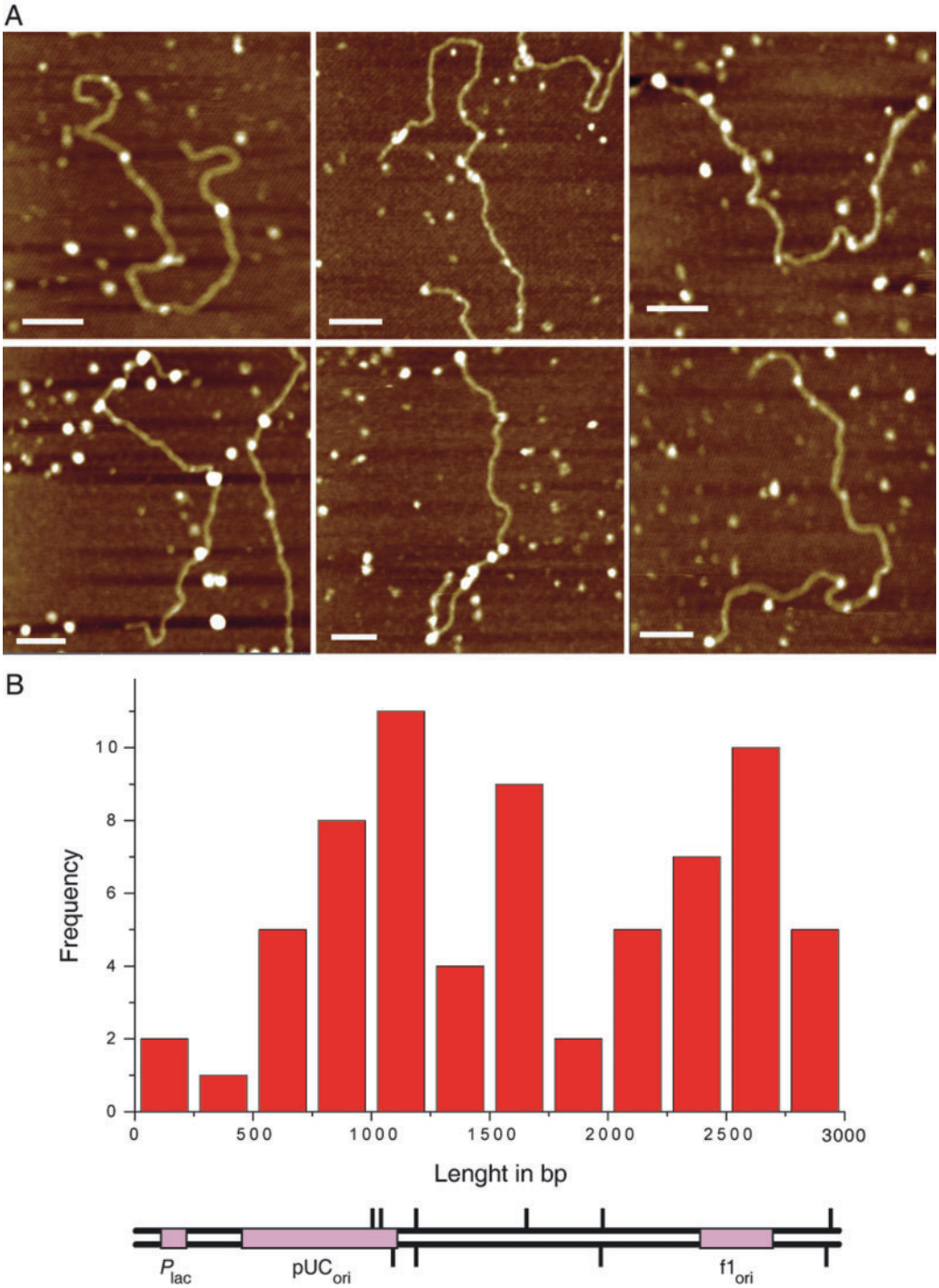

Figure 3. RecN binding to nicked DNA. Nt.AlwI-treated EcoRV-linear DNA (150 nM in nt) and RecN (10 nM) were incubated for 10 min at 37°C. Reaction was fixed with 0.1 glutaraldehyde and deposited on freshly cut mica. (**A**) AFM images of Nt.AlwI-treated DNA–RecN complexes analysed. (**B**) Geometrical analyses of Nt.AlwI-treated DNA–RecN complexes. The length from the end of the substrate to DNA-bound RecN was measured and shown as a histogram in 250 bp bin. A schematic map of plasmid DNA with the target localization for Nt.AlwI endonuclease and relevant high dA + dT regions (P_{lac}, pUC_{ori} and $f1_{ori}$) are shown at the same scale of the histogram.

number of DNA molecules that are associated with RecN complexes of different sizes. More than 20% ($n = 156$ total molecules) of the deposited molecules were found inside these structures that have a mean of five DNA molecules each (Figure 4). Similar results were observed when ATP was replaced by ADP-Mg^{2+} or ATPγS-Mg^{2+}, however rosette-like structures were not observed in the presence of AMP-PNP-Mg^{2+} (data not shown). This is consistent with previous results that AMP-PNP fails to promote CII and CIII complex formation (25).

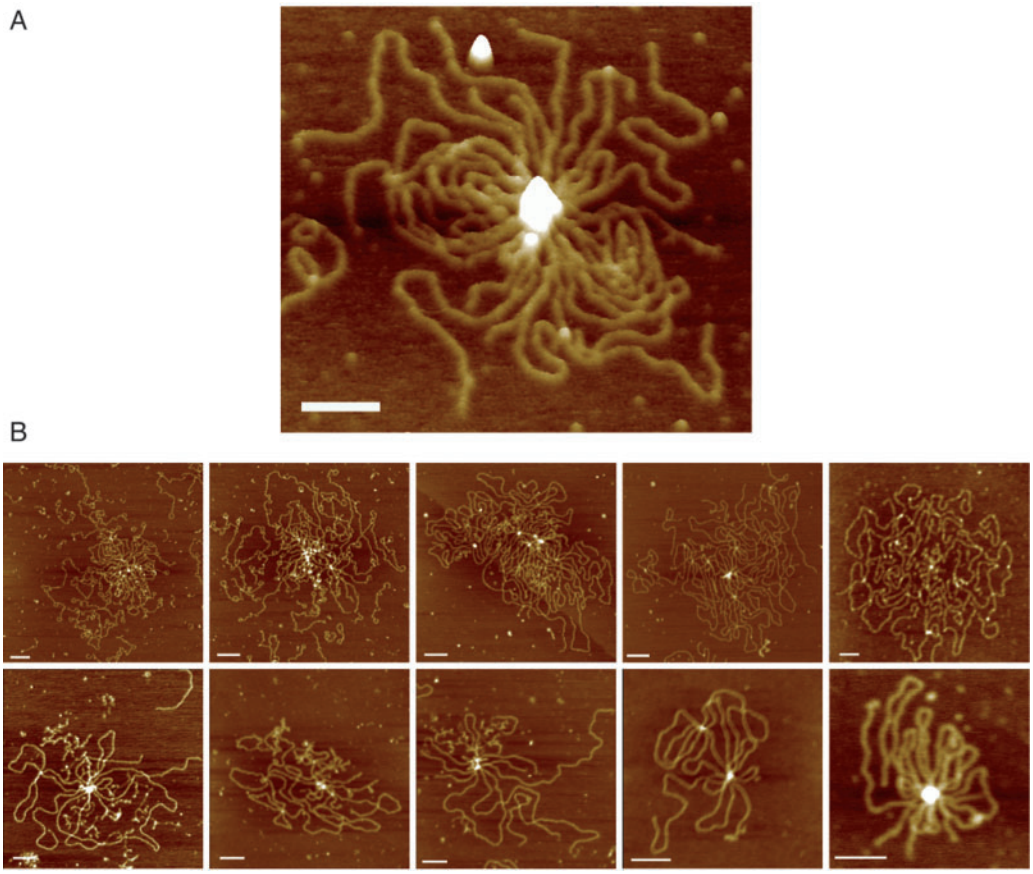

Figure 4. AFM analysis of RecN bound to DNA in presence of ATP. Linear DNA (150 nM in nt) with short ssDNA tails and RecN (10 nM) were incubated for 10 min at 37°C, then ATP (1 mM) was added and incubated for 20 min at 37°C. (**A**) 3D image of one 'rosette-like structure' stressing the height of the protein 'blob'. (**B**) Gallery of AFM images of the different species. Colour represents height from 0 to 5 nm, dark to light. Scale bar = 100 nm.

These data suggest that AMP-PNP apparently does not sufficiently promote the active form of RecN required for inter-complex assembly (rosette-like structures).

We can envisage a dynamic behaviour of RecN, with a large number of small RecN aggregates at the end of the DNA specimens (Figure 4B), and then a small number of large RecN aggregates with different DNA ends bound to it forming 'rosette-like structures' (Figure 4A).

RecA promotes disassembly of the ssDNA–RecN–ATP–Mg^{2+} complexes

In previous studies it was shown that RecA protein preferentially hydrolyses dATP than ATP, and supports an efficient DNA strand exchange in presence of dATP when compared to ATP (30,31, unpublished data). Addition of a large excess of RecA (0.2 μM), under optimized conditions for RecA binding (presence of dATP–Mg^{2+}), promoted the disassembly of the pre-formed ssDNA–RecN–dATP–Mg^{2+} (CII and CIII) complexes (25). However, the RecN–ssDNA complexes formed in the presence of dATP–Mg^{2+} (CII and CIII complexes) were not disrupted by the addition of a heterologous ssDNA-binding protein (bacteriophage SPP1 single-stranded binding protein) (25). To investigate the fate of the rosette-like structures further, EMSA experiments, under conditions optimized for RecN binding to ssDNA, were undertaken in the presence or absence of SsbA, RecA and/or 1 mM ATP or ADP. In the absence of a nucleotide, RecN bound to ssDNA to form a complex designated CI (Figure 5A, lane 2), but with ATP–Mg^{2+} or with ADP–Mg^{2+}, slower migrating RecN–ssDNA (CII and CIII) complexes were formed (Figure 5A, lanes 3 and 4 versus 2; 25).

In the presence of limiting SsbA concentration (0.15 nM), one discrete SsbA–$ssDNA_{60}$ complex was observed (5Aii, lane 14). Addition of a large excess of SsbA (100 nM) to the pre-formed CI complex was followed by the binding of SsbA to ssDNA (SsbA–ssDNA complexes, Figure 5Ai, lanes 5). ADP or ATP (denoted as NT) addition to the above reaction did not enhance CII and CIII complexes formation (Figure 5Ai, lanes 6 and 7). However, addition of SsbA (100 nM) to pre-formed ssDNA–RecN–ATP–Mg^{2+} or ssDNA–RecN–ADP–Mg^{2+} complexes failed to disassemble the CII and CIII complexes (Figure 5Aii, lanes 6 and 7). Furthermore, the ssDNA–RecN–ATP–Mg^{2+} or ssDNA–RecN–ADP–Mg^{2+} complexes or rosette-like

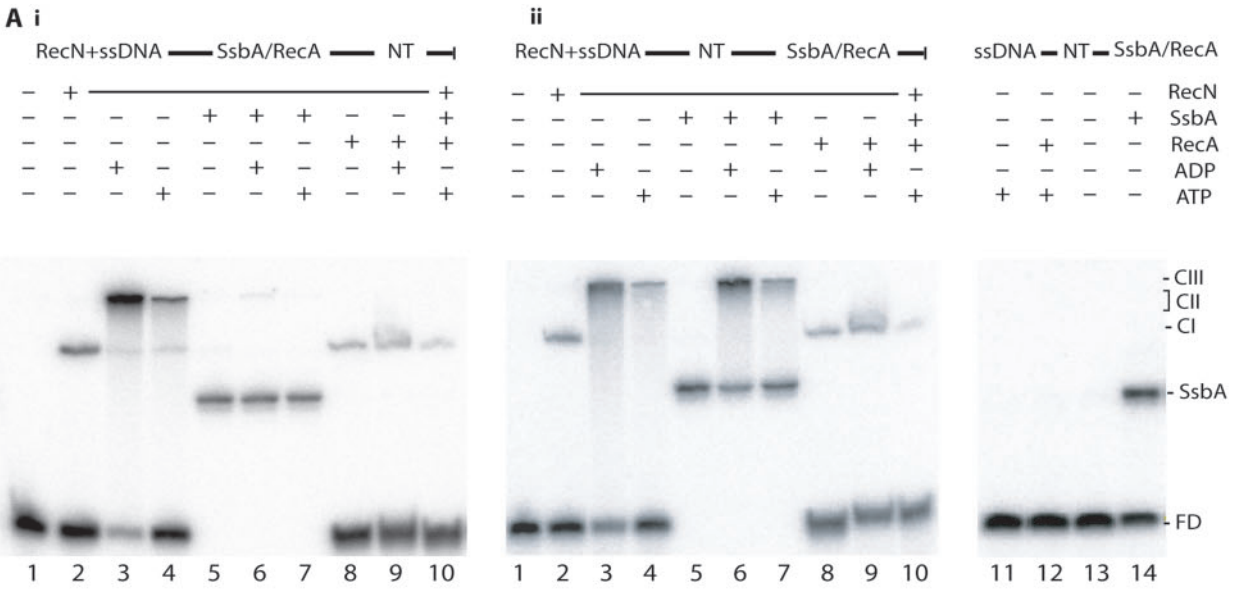
A i
RecN+ssDNA
SsbA/RecA
NT
ii
RecN+ssDNA
NT
SsbA/RecA
ssDNA
NT
SsbA/RecA
RecN
SsbA
RecA
ADP
ATP
CIII
CII
CI
SsbA
FD
1 2 3 4 5 6 7 8 9 10
1 2 3 4 5 6 7 8 9 10
11 12 13 14

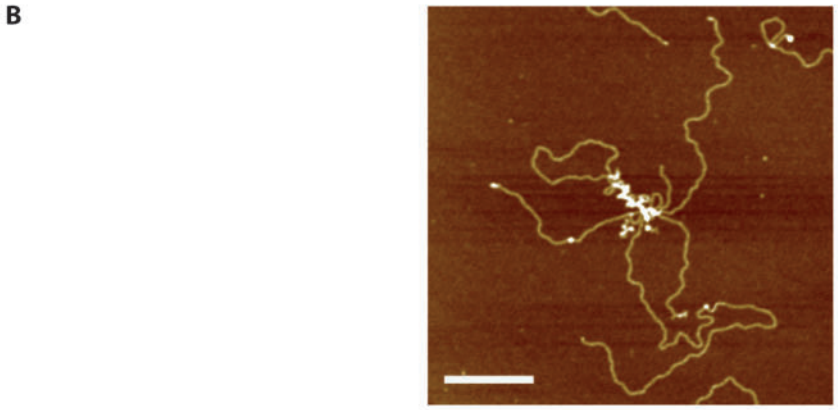
B

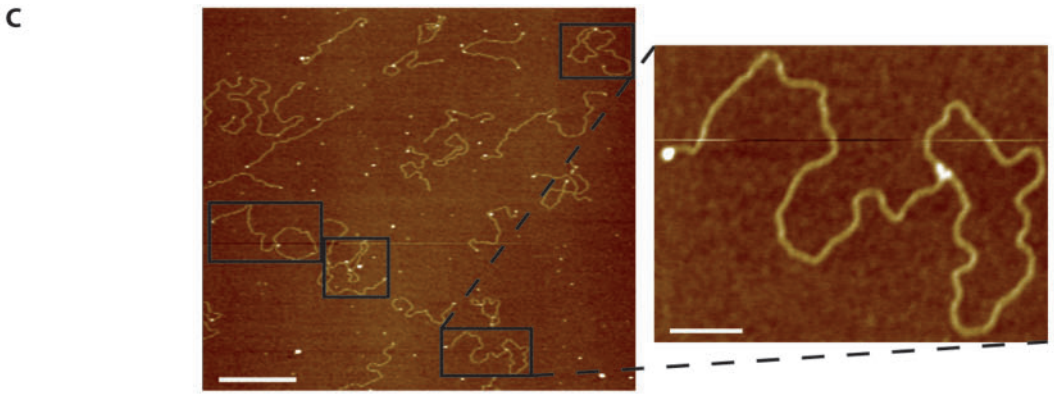
C

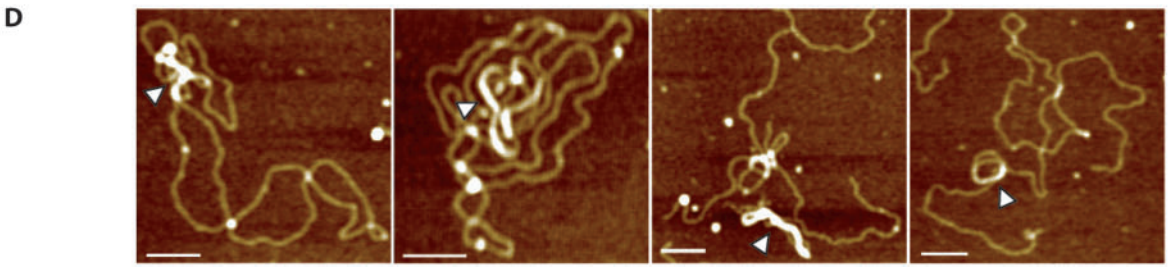
D

structures were insensitive to even 1 μM SsbA (data not shown).

Addition of sub-saturating amounts of RecA (40 nM) did not disrupt CI complexes, but in the presence of NT blocked the assembly of the slower migrating RecN–ssDNA CII and CIII complexes (5Ai, lanes 8–10) or did promote their disassembly (Figure 5Aii, lanes 8–10). Under these experimental conditions, RecA protein forms meta-stable complexes with ssDNA because complexes attributed only to ssDNA–RecA–ATP–Mg^{2+} were not observed (5Aii, lane 12). The absence of CII- and CIII-type complexes cannot be attributed to RecA-mediated hydrolysis of the ATP–Mg^{2+} because RecA promotes the disassembly of CII and CIII complexes even in the presence of ADP.

AFM visualization of RecA interactions with RecN–DNA complexes

In previous studies, it was shown that RecA-promoted pairing of homologous circular dsDNA with linear duplex with single-stranded extensions involved co-aggregation into large nucleoprotein networks (32,33; Figure 5B). To further characterize RecA interactions with ssDNA–RecN complexes, RecA-mediated DNA strand invasion complexes were visualized by AFM. In the absence of RecN, the linear duplex DNA with short ssDNA tails was pre-incubated with ATP–Mg^{2+}, and then with aliquots of homologous circular dsDNA plus sub-saturating amounts of RecA. RecA (40 nM) catalysed DNA strand invasion was observed in ~2% of total DNA molecules in a 10 min incubation time after deproteinization, but accumulation of joint molecules was not observed (<0.5%) if RecA was omitted. RecN bound to the λ Exo-generated single-stranded extensions of dsDNA molecules was pre-incubated with ATP–Mg^{2+}, and then homologous circular dsDNA plus sub-saturating amounts of RecA (40 nM) were added. RecA-mediated DNA strand invasion was observed in ~40% of total DNA molecules in a 10 min incubation time (Figure 5C).

The large rosette-like complexes seen with RecN-ATP-Mg^{2+} bound to the ssDNA tails of duplex molecules (Figure 4) were not detected in the presence of RecA. Although, RecA–DNA joint molecules were observed (Figure 5C, compare with the aggregates obtained if no RecN was added Figure 5B). These observations are consistent with RecA-promoting disassembly of the large CII- and CIII-type RecN–ssDNA complexes, and catalysing DNA strand invasion into a circular homologous dsDNA molecule in the presence of pre-formed ssDNA–RecN–ATP–Mg^{2+} complexes (Figure 5C). RecN protein fails to promote joint molecule formation in the absence of RecA protein (data not shown).

To identify which protein was bound to the joint molecule (Figure 5C), we took advantage of the fact that ATPγS–Mg^{2+} binding to RecA–ssDNA complexes promotes nucleoprotein filament formation (reviewed by 34,35). Pre-formed ssDNA–RecN–ATP–Mg^{2+} complexes were incubated with ATPγS–Mg^{2+} followed by addition of homologous circular dsDNA plus RecA. In the presence of ATPγS–Mg^{2+}, the large rosette-like complexes seen with RecN bound to ssDNA tails of duplex molecules were not detected, although long nucleoprotein filaments of RecA protein were formed at the joint molecule (Figure 5D), consistent with RecA being located at the linear-circular DNA interaction.

DISCUSSION

Different modes of RecN binding to ssDNA

Our AFM studies demonstrate that in the absence of ATP–Mg^{2+} RecN binds to ssDNA. This binding results in the formation of discrete 'blobs' on ssDNA. We did not observe preferential binding to ssDNA as compared to ssDNA within duplex DNA regions. However, in the presence of ATP–Mg^{2+} the 3′-OH DNA ends were strictly required for the formation of large ssDNA–RecN–ATP–Mg^{2+} (CII and CIII) complexes (25, Figure 5A). We observed that RecN forms also 'blobs' on nicked sites on duplex DNA, although, by EMSA experiments it was shown that in the absence of ATP–Mg^{2+} RecN forms stable complexes with ssDNA segments larger than 15-nt in length (25), thus we propose that RecN might interact with shorter ssDNA regions (e.g. nicked DNA) in a meta-stable manner.

In the presence of ATP–Mg^{2+}, the RecN–ssDNA complexes assembled to form the large CII and CIII complexes (Figure 4). It is likely that RecN bound to ssDNA translocates towards the ssDNA ends and

Figure 5. RecA interaction with ssDNA–RecN–ATP–Mg^{2+} networks. (**A**) [γ-^{32}P] $ssDNA_{60}$ (60 nM in nt) and RecN (10 nM) were pre-incubated for 10 min at 37°C in buffer C. (**Ai**) SsbA (100 nM, lanes 5–7) or RecA (40 nM, lanes 8–10) protein was added to pre-formed RecN–ssDNA complexes and incubated for 10 min at 37°C, then 1 mM ADP (lanes 6 and 9) or 1 mM ATP (lanes 7 and 10) or no nucleotide cofactor (lanes 5 and 8) was added, and incubated for 10 min at 37°C. (**Aii**) 1 mM ADP (lanes 3, 6 and 9) or 1 mM ATP (lanes 4, 7 and 10) or no nucleotide cofactor (lanes 2, 5 and 8) was added to pre-formed RecN–ssDNA complexes, and then 100 nM SsbA (lanes 5–7) or 40 nM RecA (lanes 8–10) was added and incubated for 10 min at 37°C. The protein(s)–ssDNA–NT–Mg^{2+} complexes were fractionated and visualized. In the absence of RecN, [γ-^{32}P] $ssDNA_{60}$ (60 nM in nt) was incubated with RecA (40 nM, lanes 11 and 12) or SsbA (0.15 nM, lanes 13 and 14) in presence or absence of ATP. FD, free DNA; CI, complex I; CII, complex II; CIII, complex III; NT, presence of ADP or ATP; ±, denotes presence or absence of indicated factor. The SsbA–ssDNA complex (SsbA) is indicated. (**B**) RecA–DNA aggregates in the absence of RecN. Linear DNA (150 nM) with short ssDNA tails and 40 nM RecA were incubated for 10 min at 37°C, in the presence of 1 mM ATP at 37°C. Homologous circular plasmid DNA (150 nM) was added and incubated for another 10 min at 37°C, and deposited on freshly cut mica. Scale bar = 250 nm. (**C**) RecA-promoted DNA strand invasion in presence of RecN and ATP. Linear DNA (150 nM) with short ssDNA tails and 10 nM RecN were pre-incubated for 10 min at 37°C, then 1 mM ATP was added and incubated for 10 min at 37°C. Homologous circular plasmid DNA (150 nM) and RecA protein (40 nM) were added to the pre-formed ssDNA–RecN–ATP–Mg^{2+} complex, incubated for another 10 min at 37°C, and deposited on freshly cut mica. Scale bar = 500 nm (inset picture, bar = 100 nm). (**D**) RecA-promoted DNA strand invasion in presence of RecN and ATPγS. Linear DNA (150 nM) with short ssDNA tails and RecN (10 nM) were pre-incubated for 10 min at 37°C, then 0.1 mM ATPγS was added and incubated for 10 min at 37°C. Homologous circular plasmid DNA (150 nM) and RecA protein (40 nM) were added to the pre-formed ssDNA–RecN–ATPγS–Mg^{2+} complex, incubated for another 10 min at 37°C and deposited on freshly cut mica. White arrowheads show nucleoprotein filaments of RecA and DNA. Scale bar = 100 nm.

the subunit interactions, by tethering ends, promote aggregation of different ssDNA–RecN–ATP–Mg^{2+} complexes to form a rosette-like structure. This is consistent with the observation that addition of a large excess of unlabelled ssDNA (500-fold) and ATP–Mg^{2+} to a pre-formed ssDNA–RecN complex did not reduce the formation of large nucleoprotein aggregates (25). The RecN dynamic architecture and end-binding specificity influenced by ATP–Mg^{2+} (25, this work) resemble the binding specificity of the HsRad50–Mre11–ATP–Mg^{2+} or the HsRad50–Mre11–Nbs1–ATP–Mg^{2+} complexes and also show some clear differences (25, this work, 36–38). Indeed, the Rad50–Mre11 complex, which exhibits ATP-independent dsDNA binding and such binding activity is stimulated by ATP, does not seem to bind ssDNA (39–41).

The pre-formed ssDNA–RecN–ATP–Mg^2 complexes are insensitive to the addition of SsbA, arguing that RecN should bind ssDNA prior or concomitantly with SsbA. Independent of the order of addition of sub-stoichiometric concentrations of RecA, the pre-formed ssDNA–RecN–ATP–Mg^2 (CII and CIII) complexes were disassembled or not formed. However, RecA failed to dislodge RecN from the CI complex. AFM showed that when homologous circular DNA and sub-saturating RecA concentration were incubated with pre-formed ssDNA–RecN–ATP–Mg^2 (CII–CIII) complexes RecA-promoted DNA strand invasion with more than 12-fold higher efficiency when compared to the yield of joint molecules in the absence of RecN. Under this condition, RecA should be located at the joint site of the DNA molecules, because RecA–ATPγS–Mg^{2+} is located at this site. We propose that RecA interacts with and promotes a conformational change of RecN, because the pre-formed ssDNA–RecN–ADP–Mg^{2+} complex, which is resistant to nearly saturating concentrations of chaotropic agents (25), can be disassembled by sub-stoichiometric concentrations of RecA.

The *in vivo* roles of RecN

Genetic and cytological evidence suggests that: (i) RecN and Ku/SbcC define different avenues for DSB repair (17,18,21); (ii) RecN, which plays an important role in the repair of DSBs, acts prior to and after end-processing (17,20); (iii) RecN co-localizes with RecO, RecR and RecA on the nucleoid in a majority of cells after induction of DSBs (17,21) and (iv) in the wild type background the SsbC foci mostly co-localized with the DNA polymerase complex al late times (120 min after induction of a DSB) (18). It is likely that RecN, which is ubiquitous in bacteria, provides a paradigm for the overall effect of the eukaryotic MRN(X) complex in recombination *in vivo* (42).

Do the *in vivo* foci of RecN and rosette-like structures formed *in vitro* relate directly to these repair/recombination events? The formation of RecN foci should be a multi-stepwise process, and in the bases of previous and the results presented, we proposed the following model (Figure 6). The details of this model are speculative at this point, but it is appealing because it incorporates the cytological, biochemical and structural information available: in step 1, RecN (Figure 6A) or RecN–ATP–Mg^{2+} can bind to ssDNA forming CI at gaps or CII–CIII complexes at ssDNA ends (25) as early as 15 min after DSB induction (17). In step 2, the resection of the 5′-ends of duplex DNA by RecJ in concert with a RecQ-like enzyme (RecQ and/or RecS) or the AddAB helicase–nuclease complex enhances the formation of 1 or 2 discrete RecN foci (Figure 6B). At this stage DNA end-processing, directly or indirectly, might repress the NHEJ activity and favour HR by error-free repair of DSBs (19). In the absence of both AddAB and RecJ functions many RecN foci, and absence of RecA threads were observed (20,21). In step 3, the ssDNA–RecN–ATP–Mg^{2+} complex protects the 3′-OH terminus of a DNA molecule (25), and favours ssDNA–RecN–ATP–Mg^{2+} inter-complex association, thereby increases the local concentration of ssDNA ends (Figure 6C). It is likely that RecN facilitates this process by tethering the ssDNA ends that are visualized by AFM as rosette-like structures (Figure 4), by EMSA as CII- and CIII-type complexes (25; Figure 5A) and as discrete RecN focus on the nucleoids in a majority of cells (17). We predict a dynamic behaviour of the ssDNA–RecN complexes that must be able to roam the nucleoid space in search for a discrete ssDNA–RecN–ATP–Mg^{2+} complex (RecN focus). In step 4, SsbA binds to ssDNA extensions generated by DNA end-processing (Figure 6C). The RecN rosette-like structures (CII- and CIII-type complexes) formed in step 3 cannot be disassembled by the addition of a large excess of the SsbA protein (Figure 5A), and SsbA (independent of the other of addition) partially inhibits the RecA ATPase activity (Carrasco *et al.*, unpublished data). In step 5, RecA-mediators displace SsbA from ssDNA and promote RecA loading onto ssDNA. In the absence of SsbA, RecA promotes the dislodging of the large RecN networks resulting in a large concentration of ssDNA ends (Figure 6D). Lastly, RecA polymerizes on the clustered ssDNA molecules to make pre-synaptic nucleoprotein filaments. The different RecA nucleoprotein filaments can then make single or multiple search for homology on the sister chromosome or sister strand, thus facilitating the search for genome-wide homology. This is in agreement with the observation that: (i) RecA forms foci, that co-localize with RecN, and threads or filamental structures upon DNA damage (20,43) and (ii) RecN augments RecA-mediated DNA strand invasion (Figure 5C).

Both the eukaryotic MRN(X) complex and bacterial RecN in concert with DNA end-processing functions are able to detect DNA damage, play a structural role by bridging and tethering DNA ends and may provide the structural basis for the discrimination between the different avenues of DNA repair (HR versus NHEJ) (17,18,36,37,42,this work,44,45).

SUPPLEMENTARY DATA

Supplementary Data are available at NAR Online.

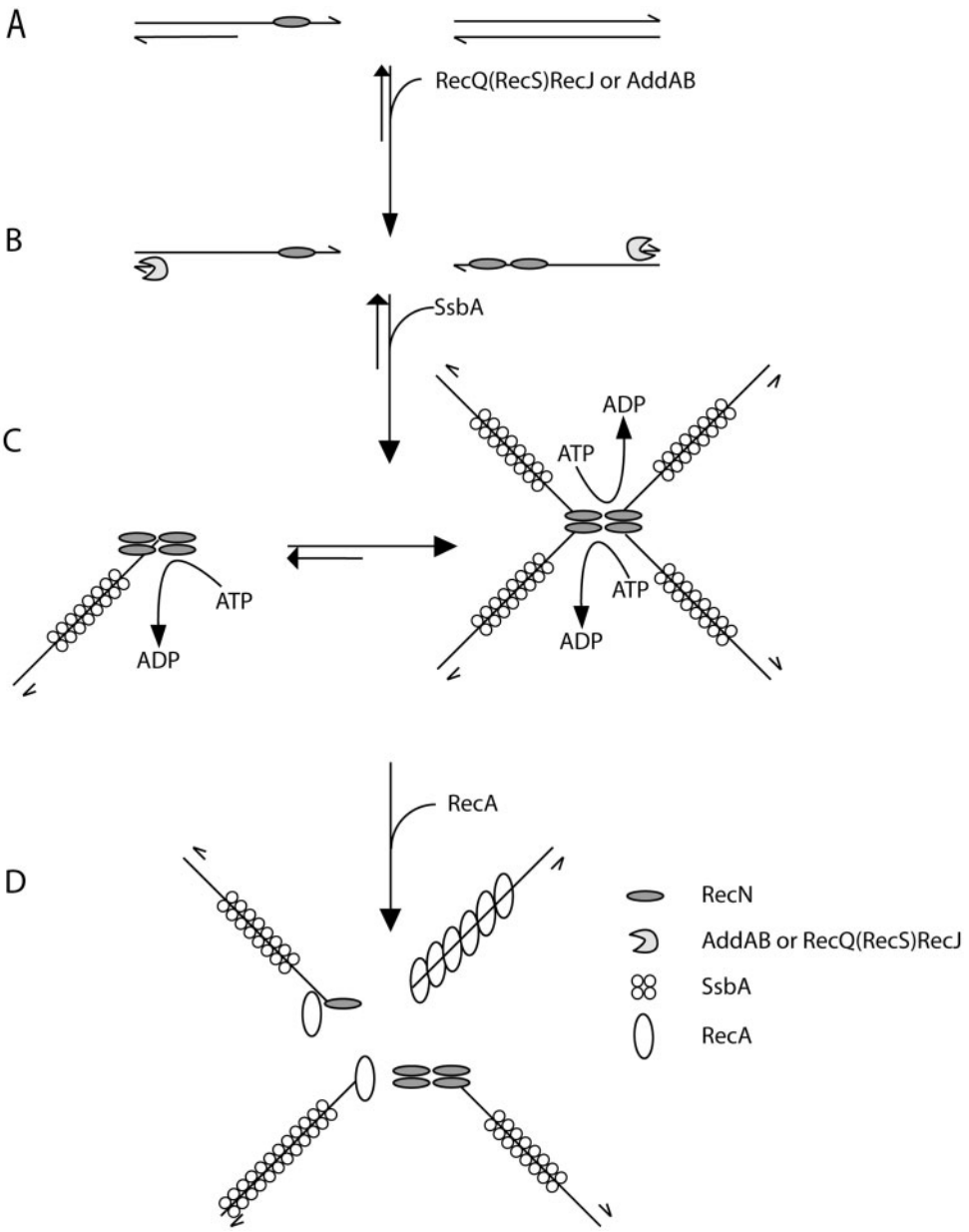

Figure 6. Mode of action of RecN protein: a proposal. RecN binds ssDNA regions of broken DNA molecule (e.g. a single-strand nick in the lagging strand template) (**A**). In the presence of ATP–Mg^{2+} and prior DNA end-processing, RecN binds to the 3′-end of ssDNA tailed duplex DNA, because it binds with high efficiency to short ssDNA segments, whereas SsbA requires patches of ssDNA longer than 35-nt. The 5′ ends of the broken DNA molecules are processed either by RecJ in concerts with a RecQ-like protein (namely RecQ or RecS) or the AddAB helicase/nuclease, resulting in a duplex molecule with a 3′-terminated ssDNA tail (**B**). After end-processing, RecN by a protein–protein and protein–ssDNA interaction forms 1 to 2 RecN foci *in vivo* and large nucleoprotein networks (rosette-like structures) *in vitro*, and SsbA binds and protects the ssDNA (**C**). RecN and RecA interaction leads to disassembly of the rosette-like structures. In the absence of SsbA, RecN helps loading RecA onto naked ssDNA and RecA polymerizes onto ssDNA to form the active RecA nucleoprotein filament formation (**D**). *In vivo* RecN directly or indirectly interacts with RecO (and perhaps RecR), and the RecA-mediators might promote the disassembly of the SsbA protein and the loading of RecA onto ssDNA. The role of the RecA-mediators remains to be unravelled.

ACKNOWLEDGEMENTS

We are very grateful to R.L. Ohniwa for valuable discussions on this work, and to L.B. Rothman-Denes, J. Reeve and C. Wyman for comments on the article. H.S. was recipient of a Fellowship of the Spanish Research Council and the Japanese Society for the Promotion of Science. This work was supported by grants BFU2006-01062 and CSD2007-00010 from Ministerio de Educación y Ciencias to J.C.A., S-0505/-MAT0283 from Comunidad de Madrid, and Grant-in-aid for Priority Area from the MEXT of Japan to K.T. Funding to pay the Open Access publication charges for this article was provided by BFU2006-01062 grant.

Conflict of interest statement. None declared.

REFERENCES

1. Bassing,C.H. and Alt,F.W. (2004) The cellular response to general and programmed DNA double strand breaks. *DNA Repair*, **3**, 781–796.
2. Krogh,B.O. and Symington,L.S. (2004) Recombination proteins in yeast. *Annu. Rev. Genet.*, **38**, 233–271.
3. Michel,B., Grompone,G., Flores,M.J. and Bidnenko,V. (2004) Multiple pathways process stalled replication forks. *Proc. Natl Acad. Sci. USA*, **101**, 12783–12788.
4. Bowater,R. and Doherty,A.J. (2006) Making ends meet: repairing breaks in bacterial DNA by non-homologous end-joining. *PLoS Genet.*, **2**, e8.
5. McGowan,C.H. and Russell,P. (2004) The DNA damage response: sensing and signaling. *Curr. Opin. Cell Biol.*, **16**, 629–633.
6. O'Driscoll,M. and Jeggo,P.A. (2006) The role of double-strand break repair—insights from human genetics. *Nat. Rev. Genet.*, **7**, 45–54.
7. Wyman,C. and Kanaar,R. (2006) DNA double-strand break repair: all's well that ends well. *Annu. Rev. Genet.*, **40**, 363–383.
8. Mirzoeva,O.K. and Petrini,J.H. (2001) DNA damage-dependent nuclear dynamics of the Mre11 complex. *Mol. Cell. Biol.*, **21**, 281–288.
9. Usui,T., Ogawa,H. and Petrini,J.H. (2001) A DNA damage response pathway controlled by Tel1 and the Mre11 complex. *Mol. Cell*, **7**, 1255–1266.
10. Lisby,M., Barlow,J.H., Burgess,R.C. and Rothstein,R. (2004) Choreography of the DNA damage response: spatiotemporal relationships among checkpoint and repair proteins. *Cell*, **118**, 699–713.
11. Stracker,T.H., Theunissen,J.W., Morales,M. and Petrini,J.H. (2004) The Mre11 complex and the metabolism of chromosome breaks: the importance of communicating and holding things together. *DNA Repair*, **3**, 845–854.
12. Lisby,M. and Rothstein,R. (2005) Localization of checkpoint and repair proteins in eukaryotes. *Biochimie*, **87**, 579–589.
13. Hopfner,K.P. and Tainer,J.A. (2003) Rad50/SMC proteins and ABC transporters: unifying concepts from high-resolution structures. *Curr. Opin. Struct. Biol.*, **13**, 249–255.
14. Connelly,J.C. and Leach,D.R. (2002) Tethering on the brink: the evolutionarily conserved Mre11-Rad50 complex. *Trends Biochem. Sci.*, **27**, 410–418.
15. Koroleva,O., Makharashvili,N., Courcelle,C.T., Courcelle,J. and Korolev,S. (2007) Structural conservation of RecF and Rad50: implications for DNA recognition and RecF function. *EMBO J.*, **26**, 867–877.
16. Hirano,T. (2002) The ABCs of SMC proteins: two-armed ATPases for chromosome condensation, cohesion, and repair. *Genes Dev.*, **16**, 399–414.
17. Kidane,D., Sanchez,H., Alonso,J.C. and Graumann,P.L. (2004) Visualization of DNA double-strand break repair in live bacteria reveals dynamic recruitment of *Bacillus subtilis* RecF, RecO and RecN proteins to distinct sites on the nucleoids. *Mol. Microbiol.*, **52**, 1627–1639.
18. Mascarenhas,J., Sanchez,H., Tadesse,S., Kidane,D., Krishnamurthy,M., Alonso,J.C. and Graumann,P.L. (2006) *Bacillus subtilis* SbcC protein plays an important role in DNA inter-strand cross-link repair. *BMC Mol. Biol.*, **7**, 20.
19. Weller,G.R., Kysela,B., Roy,R., Tonkin,L.M., Scanlan,E., Della,M., Devine,S.K., Day,J.P., Wilkinson,A. *et al.* (2002) Identification of a DNA nonhomologous end-joining complex in bacteria. *Science*, **297**, 1686–1689.
20. Kidane,D. and Graumann,P.L. (2005) Dynamic formation of RecA filaments at DNA double strand break repair centers in live cells. *J. Cell Biol.*, **170**, 357–366.
21. Sanchez,H., Kidane,D., Cozar,M.C., Graumann,P.L. and Alonso,J.C. (2006) Recruitment of *Bacillus subtilis* RecN to DNA double-strand breaks in the absence of DNA end processing. *J Bacteriol.*, **188**, 353–360.
22. Hahn,J., Maier,B., Haijema,B.J., Sheetz,M. and Dubnau,D. (2005) Transformation proteins and DNA uptake localize to the cell poles in *Bacillus subtilis*. *Cell*, **122**, 59–71.
23. Kidane,D. and Graumann,P.L. (2005) Intracellular protein and DNA dynamics in competent *Bacillus subtilis* cells. *Cell*, **122**, 73–84.
24. Petrini,J.H. and Stracker,T.H. (2003) The cellular response to DNA double-strand breaks: defining the sensors and mediators. *Trends Cell Biol.*, **13**, 458–462.
25. Sanchez,H. and Alonso,J.C. (2005) *Bacillus subtilis* RecN binds and protects 3'-single-stranded DNA extensions in the presence of ATP. *Nucleic Acids Res.*, **33**, 2343–2350.
26. Carrasco,B., Ayora,S., Lurz,R. and Alonso,J.C. (2005) *Bacillus subtilis* RecU Holliday-junction resolvase modulates RecA activities. *Nucleic Acids Res.*, **33**, 3942–3952.
27. Nettikadan,S., Tokumasu,F. and Takeyasu,K. (1996) Quantitative analysis of the transcription factor AP2 binding to DNA by atomic force microscopy. *Biochem. Biophys. Res. Commun.*, **226**, 645–649.
28. Hizume,K., Yoshimura,S.H. and Takeyasu,K. (2005) Linker histone H1 per se can induce three-dimensional folding of chromatin fiber. *Biochemistry*, **44**, 12978–12989.
29. Lohman,T.M. and Ferrari,M.E. (1994) *Escherichia coli* single-stranded DNA-binding protein: multiple DNA-binding modes and cooperativities. *Annu. Rev. Biochem.*, **63**, 527–570.
30. Lovett,C.M.Jr. and Roberts,J.W. (1985) Purification of a RecA protein analogue from *Bacillus subtilis*. *J. Biol. Chem.*, **260**, 3305–3313.
31. Steffen,S.E. and Bryant,F.R. (1999) Reevaluation of the nucleotide cofactor specificity of the RecA protein from *Bacillus subtilis*. *J. Biol. Chem.*, **274**, 25990–25994.
32. Gonda,D.K. and Radding,C.M. (1986) The mechanism of the search for homology promoted by RecA protein. Facilitated diffusion within nucleoprotein networks. *J. Biol. Chem.*, **261**, 13087–13096.
33. Pinsince,J.M. and Griffith,J.D. (1992) Early stages in RecA protein-catalyzed pairing. Analysis of coaggregate formation 0and non-homologous DNA contacts. *J. Mol. Biol.*, **228**, 409–420.
34. Kowalczykowski,S.C. and Eggleston,A.K. (1994) Homologous pairing and DNA strand-exchange proteins. *Annu. Rev. Biochem.*, **63**, 991–1043.
35. Lusetti,S.L. and Cox,M.M. (2002) The bacterial RecA protein and the recombinational DNA repair of stalled replication forks. *Annu. Rev. Biochem.*, **71**, 71–100.
36. de Jager,M., van Noort,J., van Gent,D.C., Dekker,C., Kanaar,R. and Wyman,C. (2001) Human Rad50/Mre11 is a flexible complex that can tether DNA ends. *Mol. Cell*, **8**, 1129–1135.
37. de Jager,M., Wyman,C., van Gent,D.C. and Kanaar,R. (2002) DNA end-binding specificity of human Rad50/Mre11 is influenced by ATP. *Nucleic Acids Res.*, **30**, 4425–4431.
38. Moreno-Herrero,F., de Jager,M., Dekker,N.H., Kanaar,R., Wyman,C. and Dekker,C. (2005) Mesoscale conformational changes in the DNA-repair complex Rad50/Mre11/Nbs1 upon binding DNA. *Nature*, **437**, 440–443.
39. Raymond,W.E. and Kleckner,N. (1993) RAD50 protein of *S. cerevisiae* exhibits ATP-dependent DNA binding. *Nucleic Acids Res.*, **21**, 3851–3856.
40. Paull,T.T. and Gellert,M. (1999) Nbs1 potentiates ATP-driven DNA unwinding and endonuclease cleavage by the Mre11/Rad50 complex. *Genes Dev.*, **13**, 1276–1288.
41. Hopfner,K.P., Karcher,A., Shin,D.S., Craig,L., Arthur,L.M., Carney,J.P. and Tainer,J.A. (2000) Structural biology of Rad50 ATPase: ATP-driven conformational control in DNA double-strand break repair and the ABC-ATPase superfamily. *Cell*, **101**, 789–800.
42. Sanchez,H., Carrasco,B., Ayora,S. and Alonso,J.C. (2007) *Dynamics of DNA Double-Strand Break Repair in Bacillus subtilis*. Horizon Scientific Press, Norwich.
43. Levin-Zaidman,S., Frenkiel-Krispin,D., Shimoni,E., Sabanay,I., Wolf,S.G. and Minsky,A. (2000) Ordered intracellular RecA-DNA assemblies: a potential site of *in vivo* RecA-mediated activities. *Proc. Natl Acad. Sci. USA*, **97**, 6791–6796.
44. Costanzo,V., Paull,T., Gottesman,M. and Gautier,J. (2004) Mre11 assembles linear DNA fragments into DNA damage signaling complexes. *PLoS Biol.*, **2**, E110.
45. Lobachev,K., Vitriol,E., Stemple,J., Resnick,M.A. and Bloom,K. (2004) Chromosome fragmentation after induction of a double-strand break is an active process prevented by the RMX repair complex. *Curr. Biol.*, **14**, 2107–2112.